Applied Radiation and Isotopes 147 (2019) 136–143

Contents lists available at ScienceDirect

Applied Radiation and Isotopes

journal homepage: www.elsevier.com/locate/apradiso

Neutron spectrum unfolding using three artificial intelligence optimization methods

Jie Wang*, Yulin Zhou, Zhirong Guo, Haifeng Liu

Wuhan Second Ship Design and Research Institute, Wuhan, 430064, China

HIGHLIGHTS

- Three artificial intelligence methods are described and optimized.
- Sixty-three spectra are unfolded with use of three artificial intelligence optimization methods.
- The three optimization methods can effectively unfold neutron spectra.
- The generalized regression neural network method is the fastest and most accurate among the three methods.

ARTICLE INFO

Keywords:
Neutron spectrum unfolding
Radial basis function neural networks
Genetic algorithms
Generalized regression neural networks

ABSTRACT

Many methods have been proposed and developed in research into neutron spectrum unfolding. In this work, three artificial intelligence optimization methods—genetic algorithms, radial basis function neural networks and generalized regression neural networks—were developed on the basis of former research to retrieve the neutron spectrum. Sixty-three neutron spectra were unfolded on the basis of the same response functions with the three methods, and three indexes—the mean squared error, the spectral quality and the sphere reading quality—were applied with the aim to compare the generalized unfolding performance. The results obtained with the three methods show that the unfolded neutron spectra are mostly acceptable using three methods without the initial guess spectra and that the generalized regression neural network method is the fastest and most accurate method with the most powerful generalization ability.

1. Introduction

Neutron spectrometry is of great importance in the nuclear and reactor research fields, especially the specific neutron energy distribution information provided can be used to select the proper survey instruments in the field of neutron radiation dosimetry. Bonner sphere spectrometry (BSS), which was first introduced by Bramblett et al. (1960), has been widely applied as an effective form of neutron spectrometry spanning the wide energy range from thermal to gigaelectronvolt neutrons (Thomas and Alevra, 2002). BSS, also commonly known as multisphere neutron spectroscopy, involves the use of a thermal neutron detector placed at the center of a set of different high-density polyethylene moderating spheres with different diameters (Hsu et al., 1994; Mares and Schraube, 1994; Bedogni et al., 2008). Nevertheless, BSS has some drawbacks, such as the heavy weight of the measurement sets and the complex and time-consuming operation (Vega-Carrillo, 2002). More recently, some alternative designs have been proposed and developed that embed multiple thermal neutron detectors arranged along the three mutually orthogonal axes of a single moderator sphere (Toyokawa et al., 1997; Yamaguchi et al., 1999). The spectrometric information can be derived from measurements with a single-sphere spectrometry in a single exposure (Lis et al., 2008a, b; Gomez-Ros et al., 2010, 2012). A single-sphere spectrometer could be designed as a real-time neutron spectrometer to obtain the time-dependent neutron spectra (Bedogni et al., 2014; Hoshor et al., 2015).

Measurements by BSS or single-sphere spectrometry (SSS) cannot give directly the neutron spectrum without the unfolding process, and so many unfolding methods have been studied and optimized to obtain better neutron spectra (Reginatto, 2010), such as matrix inversion and singular value decomposition methods (Jaynes, 1984), Monte Carlo methods (Sanna and Brien, 1971), regularization methods (Frieden, 1988; Routti and Sandberg, 1980), least-squares spectrum adjustments (Matzke, 2003), parameter estimations, iterative unfolding methods (Bedogni et al., 2007), and the maximum entropy principle (Shore and

* Corresponding author.
E-mail address: 1091629887@qq.com (J. Wang).

https://doi.org/10.1016/j.apradiso.2019.03.009
Received 7 September 2018; Received in revised form 22 February 2019; Accepted 4 March 2019
Available online 07 March 2019
0969-8043/

Johnson, 1980; Reginatto et al., 2002). With the development of artificial intelligence (AI) algorithms, new methods based on genetic algorithms (GAs) and artificial neural networks (ANNs) have been applied to solve the neutron spectrum unfolding problem.

GAs were first introduced by John Holland to mimic natural evolution of living systems on the basis of the concept of the "survival of the fittest" (Freeman et al., 1999; Reginatto, 2010). The basic principle of GAs is to search for the highest-fitness individual within a population through evolution and consists of four basic operations: random initial population generation, random pairing selection, preferential mating, and introduction of a new genetic mutation. For application to neutron spectrum unfolding, candidate neutron spectra can be treated as the potential individuals and the value of each candidate spectrum within the group of solutions is judged by agreement between the calculated count rate and the count rate measured by BSS or SSS. Successive generation involving the four basic processes collectively leads to better spectra with better fitness values. However, most previous research applied GAs for unfolding only a few typical neutron spectra, and the generalization to neutron spectrum unfolding is hard to achieve (Mukherjee, 1999; Santos et al., 2012; Suman and Sarkar, 2014; Shahabinejad et al., 2016).

Neural networks are computational models generated from the biological nervous system for learning and optimization. They can simulate complex relationships between inputs and outputs by learning and training to associate known inputs with the corresponding outputs. The adaptive system can change its structure by adjusting internal parameters so that the error between the computed outputs and the expected outputs is minimal for all samples (input-output pairs) used in the learning process. Once the learning and the training processes have been accomplished, an appropriate output is given corresponding to the new input presented by the network user (Braga and Dias, 2002; Kardan et al., 2003). For application to neutron spectrum unfolding, the inputs are a set of count rates from BSS or SSS and the outputs are a set of corresponding neutron spectra. Most previous work using ANNs based on multilayer perceptron networks to solve the neutron spectrum unfolding problem focused on backpropagation neural networks (BPNNs). The unfolding results are good but the disadvantage is that the BPNN method requires huge amounts of neutron spectrum data to train and test the networks, and thus the time required is relatively long (Kardan et al., 2004; Vega-Carrillo et al., 2009).

Radial basis function (RBF) neural networks are ANNs that use RBFs as activation functions. In general, RBF neural networks consist of three layers with feed-forward structures: input layer, hidden layer, and output layer. A nonnegative nonlinear RBF, mainly a Gaussian kernel function, is built in the hidden layer to map the input into the space of the hidden layer, and the output layer is a linear combination of outputs from hidden-layer RBFs and weights that are to be determined. Recently, RBF neural networks, in which a neuron is added to the hidden layer after each epoch until the specified goal has been achieved, have been successfully applied for unfolding of neutron spectra obtained with LiI detectors with Eu impurity and show better unfolding performance than multilayer perceptron neural networks. However, their use results in some negative values, which are not physically acceptable in neutron spectra (Alvar et al., 2017).

Generalized regression neural networks (GRNNs) were first introduced by Specht (1991). As a branch of RBF neural networks, GRNNs are feed-forward neural networks based on nonlinear regression theory. GRNNs are different from RBFs in the weights connecting the hidden layer with the output layer. In the case of GRNNs, the outputs are directly chosen as the weights to avoid many adjustments in the iterative process, which makes it faster. Martinez-Blanco et al. (2016) presented a computational tool based on GRNNs that is much faster to train and more accurate than BPNNs in the prediction of neutron spectra.

The main aim of this work is to unfold the neutron spectra using three optimization methods based on AI algorithms: GAs, RBF neural networks, and GRNNs. The computational codes were all developed in the MATLAB programming environment (MATLAB and Statistics Toolbox Release 2009a). Two hundred fifty-one neutron spectra from the International Atomic Energy Agency (IAEA) compendium (IEAE, 2001) were used to train and test the RBF neural networks and GRNNs. To assess the performance of the three methods, a four-fold cross validation was applied. One-fourth of the 251 neutron spectra were randomly chosen as the expected spectra in the GA method and the test spectra in the RBF neural networks and GRNN methods, and the other three-fourths of the neutron spectra were used to train the RBF neural network and the GRNNs, and also played the role of reference spectra in the GA method. The three effective and optimized AI methods are compared with regard to unfolding of sixty-three neutron spectra for the first time.

2. Materials and methods

In the neutron spectrum unfolding process, the homogeneous Fredholm integral equation theoretically characterizes the relation between the neutron energy spectrum $\varphi(E)$, the response function $R_j(E)$, and the count rate reading C_j of the jth moderator sphere:

$$C_j = \int_0^\infty R_j(E)\varphi(E)dE, \quad j = 1,2, \ldots, m. \tag{1}$$

In practice, the response function of the jth moderator sphere $R_j(E)$ is usually obtained by simulation computation as an n-dimensional vector, where n is the number of energy groups. Eq. (1) may thus be approximated as a discrete form:

$$C_j = \sum_{i=1}^{n} R_{ij}\varphi_i, \quad j = 1,2, \ldots, m. \tag{2}$$

The number of energy groups n is much larger than the number of sphere measurements m, which leads to a underdetermined problem and an infinite number of solutions. The art of unfolding is to determine the only solution as close as possible to the actual neutron energy spectrum.

The response matrix R in this work was extracted from data calculated by Physikalisch-Technische Bundesanstalt (PTB) using ^{3}He-filled Bonner spheres (Wiegerl et al., 1994; IEAE, 2001). Taking the diversity of response vectors into consideration, the following eight sets were used: a bare sphere and 2.5-, 3.5-, 5-, 7-, 9.5-, 12-, 15-in spheres. The response matrix is plotted in Fig. 1.

The three AI optimization methods automate the following preprocessing:

- Read the response matrix composed of eight response vectors. Considering that the elements of the response matrix in last seven energy groups are nulls, only the elements of the response matrix in

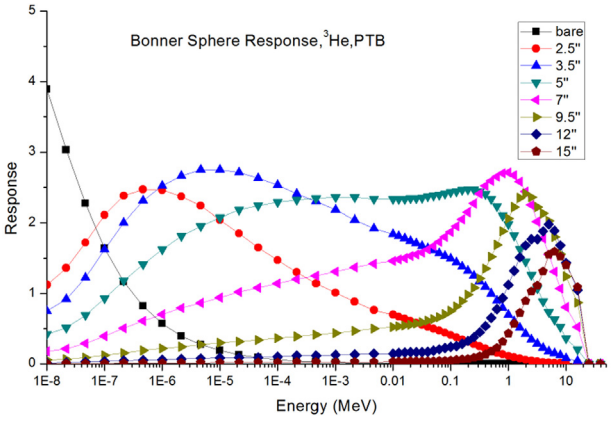

Fig. 1. Responses of ^{3}He-filled Bonner spheres from Physikalisch-Technische Bundesanstalt (PTB).

fifty-three out of sixty energy groups are used.

- Read the 251 neutron spectra in 53 energy groups from the IAEA compendium.
- Convert the neutron spectra in lethargy units to neutron spectra in energy units.
- Calculate the count rates using neutron spectra in energy units multiplied by the response matrix, and use them as the measured count rates.
- Select randomly one-fourth of neutron spectra (i.e., 63 spectra) as the expected target spectra based on four-fold cross validation to compare the unfolding performance of the three AI optimization methods.

2.1. Genetic algorithms

The GA optimization method was applied for neutron spectrum unfolding. The first step of the GAs is to define the candidate solution vectors $\varphi = <\varphi(1), \varphi(2), ..., \varphi(i), ..., \varphi(N)>$, where N is 53, the same as the number of energy groups. Determination of the solution space is especially important because a large search space will make the computation extremely time-consuming. The neutron spectrum is physically a nonnegative distribution, and thus the lower bound of the solution space is set to zero, $\varphi_{min}(i) = 0$. The upper bound is partially determined on the basis of the method proposed by Freeman et al. (1999). The eight-group scaling method is applied to divide the 53 energy groups into eight coarse groups. Combined with eight sphere readings, a full defined 8×8 matrix will be created. The eight-group scaling method maintains the profiles of the original φ_{max}^{53} within each energy group and normalizes the integral spectra over the eight coarse broad energy groups to match φ_{max}^{8}:

$$\varphi_{max}(i) = \left(\frac{\varphi_{max}^{8}(k)}{\sum_{i=E_L}^{E_U} \varphi_{max}^{53}(i)} \right) \varphi_{max}^{53}(i), \quad k = 1,2, ...,8, \quad i = 1,2, ...,53, \tag{3}$$

where k is the coarse energy group structure, and E_L and E_U are, respectively, the lower and upper energy bounds of the corresponding coarse energy groups.

However, the use of the eight-group scaling method is not sufficient to reduce the solution search spaces. The remaining three-fourths of the spectra can be used as reference spectra to provide a semiempirical maximum value $\varphi_{max}^{ref}(i)$. If $\varphi_{max}(i)$ is twice as large as $\varphi_{max}^{ref}(i)$, the latter is used instead. The search solution space is completely defined as above.

A population of 188 neutron spectrum vectors randomly generated in the solution space were initialized as the first generation. After the initial population had been specified, each spectrum vector as an individual within the population was evaluated by fitness or cost. The maximum fitness corresponds to the minimum cost. The cost is defined as

$$cost = cost_{CR} + \alpha cost_{SM} + \beta cost_{RS}. \tag{4}$$

$cost_{CR}$ is the cost from the error of measured count rates and calculated count rates deduced from the candidate spectrum vectors and the response matrix, and it is defined as

$$cost_{CR} = \sum_{j=1}^{8} \left(\frac{C_{cal,j} - C_{meas,j}}{C_{meas,j}} \right)^2. \tag{5}$$

$cost_{SM}$ is the cost from the smoothness of the solution, and the weight of smoothness α is set to 0.1. Except for some extreme cases, the neutron spectrum is a smooth and continuous distribution. $cost_{SM}$ is defined as

$$cost_{SM} = \frac{1}{2} \left[\sum_{i=2}^{53} (\varphi_i - \varphi_{i-1})^2 + \sum_{i=2}^{52} (\varphi_{i-1} - 2\varphi_i + \varphi_{i+1})^2 \right]. \tag{6}$$

$cost_{RS}$ is the cost from the difference between the calculated spectrum and a reference spectrum from 188 spectra and the corresponding coefficient $\beta = 0.1$. The idea is based on the expectation of the existence of a similar spectrum among the 188 spectra, $cost_{RS}$ is defined as

$$cost_{RS} = \min \left\{ \sum_{i=1}^{53} \frac{\varphi(i) - \varphi_{ref}(i)}{\varphi_{ref}(i)} \right\}. \tag{7}$$

In the selection step, random pairing techniques were used to select parents, and mating was frequently performed among the parents selected with high fitness to reproduce offspring in each generation with a probability $P_c = 0.7$. P_c is commonly between 0.5 and 0.9; lower P_c leads to slow convergence and a higher value results in unwanted distortion. Iterative mutation was introduced where a few spectra from the solutions were picked randomly and were improved with mutation probability $P_m = 0.01$; a smaller value of P_m leads to quicker convergence of the algorithm. After the mating and mutation processes, the resulting spectra were evaluated by the fitness. The unfit spectra were removed from the solution spectra and the elites were carried forward to the next generation. The evolutionary process of parent selection, mating, mutation, and fitness evaluation was repeated with the new generations until the maximum number of generations. Hence the cost must converge to the minimum value after a number of generations. Fig. 2 shows a semilog plot of the cost in each generation for all 63 test spectra. Convergence is evident when the maximum number of generations is 500. The computational time is 2679 s for 63 spectra (i.e., about 42 s on average for each spectrum unfolding).

2.2. Radial basis function neural networks

RBF neural networks can generally be classified into two categories according the number of neurons in the hidden layer. In one category a neuron is added to the hidden layer of an RBF neural network after each epoch until it meets the specified goal, as done by Alvar et al. (2017). In the other category the number of neurons in the hidden layer is chosen to be the same as the number of samples in the training process, as done in this work.

The spread constant greatly influences the performance of RBF neural networks. The leave-one-out cross validation technique was applied to optimize the spread constant for neural networks. Each single spectrum from the 251 original spectra was selected as the test spectrum and the remaining spectra were used as the training spectra. The spread constant was varied from 0 to 2 in increments of 0.01. To assess the performance in each fold, the mean value of the mean squared error (MSE) in Eq. (8), the mean value of the spectral quality Q_s in Eq. (9), and the mean value of the sphere reading quality Q_r in Eq.

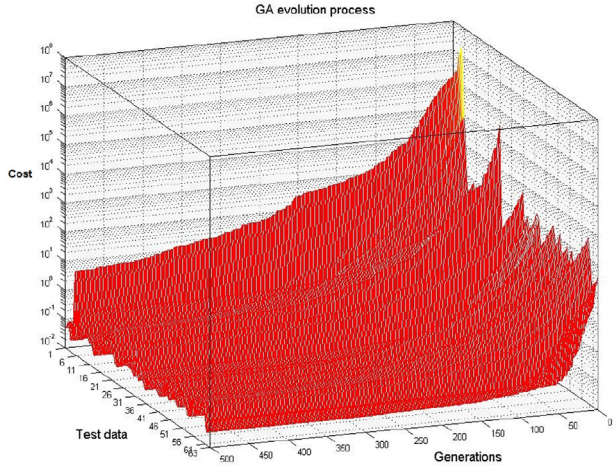

Fig. 2. Semilog plot of the cost in each generation for all 63 test spectra in the genetic algorithm (GA) evolution process.

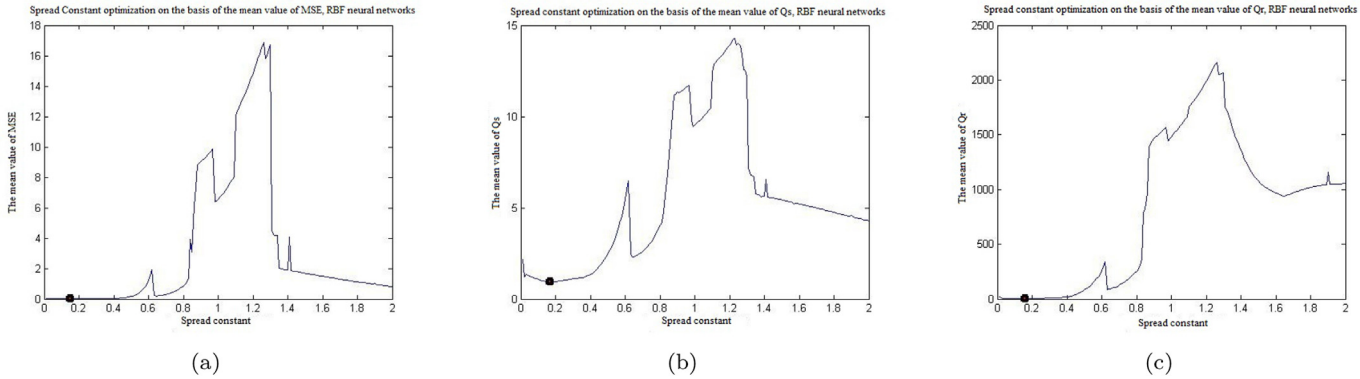

Fig. 3. The mean values of three performance indexes of 251 spectra with respect to spread constants in the range from 0.01 to 2 in increments of 0.01. (a) The marked optimum spread constant of 0.15 corresponds to the minimal mean value of the mean squared error (MSE). (b) The marked optimum spread constant of 0.17 corresponds to the minimal mean value of the spectral quality Q_s. (c) The marked optimum spread constant of 0.16 corresponds to the minimal mean value of the sphere reading quality Q_r. RBF neural networks, radial basis function neural networks.

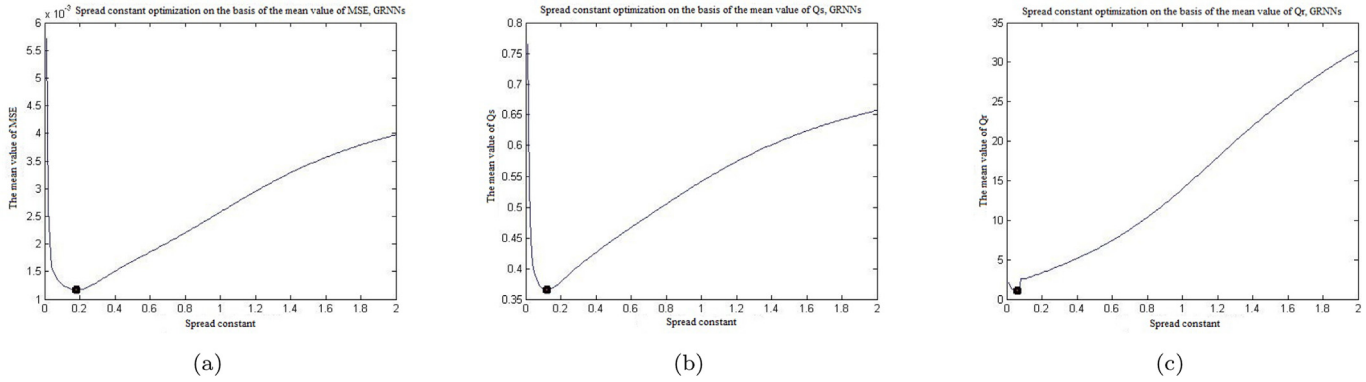

Fig. 4. The mean values of three performance indexes of 251 spectra with respect to spread constants in the range from 0.01 to 2 in increments of 0.01. (a) The marked optimum spread constant of 0.18 corresponds to the minimal mean value of the mean squared error (MSE). (b) The marked optimum spread constant of 0.12 corresponds to the minimal mean value of the spectral quality Q_s. (c) The marked optimum spread constant of 0.06 corresponds to the minimal mean value of the sphere reading quality Q_r. GRNNs, generalized regression neural networks.

Table 1
Performance of the genetic algorithm (GA) method with the multiseed averaging technique.

Seed number	Mean MSE	Mean Q_s	Mean Q_r
1	2.3×10^{-3}	0.5811	0.0621
2	2.6×10^{-3}	0.5904	0.0623
3	2.5×10^{-3}	0.5884	0.0604
4	2.4×10^{-3}	0.5994	0.0650
5	2.4×10^{-3}	0.5883	0.0662
Average spectrum	2.1×10^{-3}	0.5175	0.0620

(10) of 251 spectra were calculated and are plotted in Fig. 3. The optimum spread constant is 0.15 on the basis of the minimal mean value of MSE, 0.17 on the basis of the minimal mean value of Q_s, and 0.16 on the basis of the minimal mean value of Q_r. The total computational time was 4857 s for 50,200 (200 spread constants × 251 spectra) neural networks, with each neural network requiring 0.096 s on average.

2.3. Generalized regression neural networks

Similarly to RBF neural networks, the spread constant influences the generalization capability and is the only parameter of GRNNs. The same technique was applied to determine the spread constant. The mean value of MSE, the mean value of Q_s, and the mean value of Q_r were calculated and are plotted in Fig. 4. The optimum spread constant is 0.18 on the basis of the minimal mean value of MSE, 0.12 on the basis of the minimal mean value of Q_s, and 0.06 on the basis of the minimal mean value of Q_r. The total computational time was 639 s for 50,200 neural networks, with each neural network requiring 0.0127 s on average. The GRNN method is almost eight times faster than the RBF method and four times faster than the GA method in the preprocessing.

3. Results

MSE, Q_s, and Q_r were used to assess the unfolding performance. MSE and Q_s are mostly used to measure how closely the unfolded spectrum matches the target spectrum in each energy group, and Q_r characterizes the ability to reproduce measured sphere readings. A perfect unfolded spectrum matches the actual expected spectrum, producing MSE and Q_s equal to zero, and the calculated readings are exactly the same as the measured sphere readings, producing Q_r equal to zero. The respective formula are as follows

$$\mathrm{MSE}=\frac{1}{53}\sum_{i=1}^{53}\left[\varphi_{cal}(i)-\varphi_{act}(i)\right]^2, \tag{8}$$

$$Q_s=\left[\frac{\sum_{i=1}^{53}\left[\varphi_{cal}(i)-\varphi_{act}(i)\right]^2}{\sum_{i=1}^{53}\varphi_{act}(i)^2}\right]^{1/2}, \tag{9}$$

$$Q_r=\left[\frac{1}{8}\sum_{j=1}^{8}\left(\frac{C_{cal}(j)-C_{meas}(j)}{C_{cal}(j)}\right)^2\right]^{1/2}. \tag{10}$$

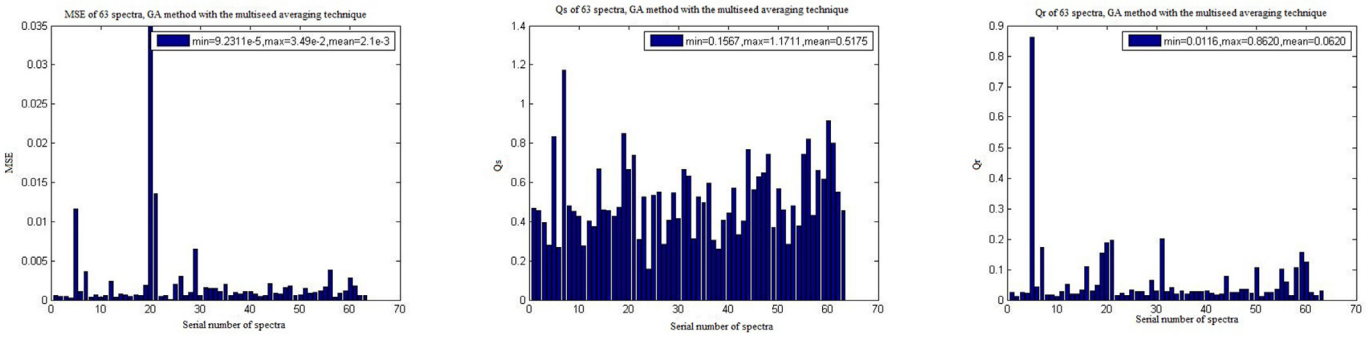

Fig. 5. Performance indexes of 63 spectra obtained by the genetic algorithm (GA) method with the multiseed averaging technique plotted as bar graphs. (a) For the mean squared error (MSE), the minimum is 9.2311×10^{-5}, the maximum is 3.49×10^{-2}, and the mean is 2.1×10^{-3}. (b) For the spectral quality Q_s, the minimum is 0.1567, the maximum is 1.1711, and the mean is 0.5175. (c) For the sphere reading quality Q_r, the minimum is 0.0116, the maximum is 0.8620, and the mean is 0.0620.

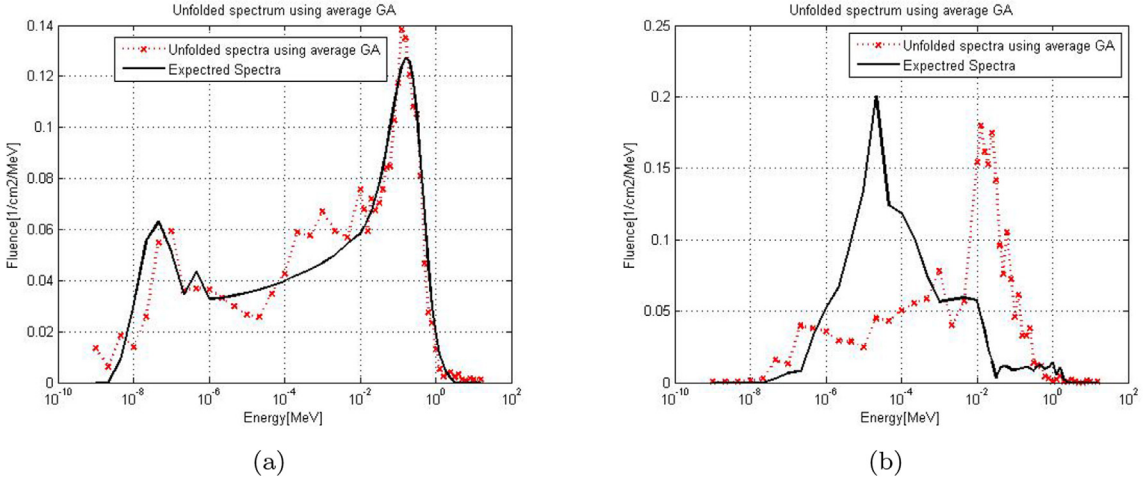

Fig. 6. (a) The best unfolded spectrum obtained by the genetic algorithm (GA) method with the multiseed averaging technique (dotted red line) and the corresponding actual expected spectrum (continuous black line). (b) The worst unfolded spectrum (dotted red line) and the corresponding actual expected spectrum (continuous black line). (For interpretation of the references to colour in this figure legend, the reader is referred to the Web version of this article.)

Table 2
Performance of the radial basis function (RBF) neural network method.

Space constraints	Mean MSE	Mean Q_s	Mean Q_r
No	6.1×10^{-3}	0.9637	11.6525
Yes	2.8×10^{-3}	0.5830	11.011

3.1. GA results

Sixty-three spectra were unfolded with the GA optimization method with the multiseed averaging technique. Each spectrum was unfolded five times on the basis of different seeds, and an average spectrum was calculated by our averaging these five calculated spectra in each energy

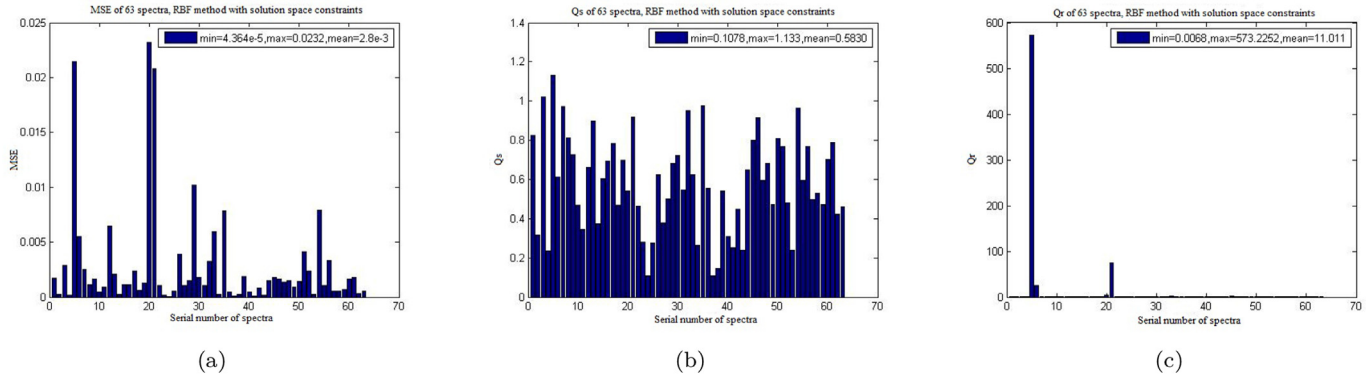

Fig. 7. Performance indexes of 63 spectra obtained by the radial basis function (RBF) method with solution space constraints. (a) For the mean squared error (MSE), the minimum is 4.364×10^{-5}, the maximum is 0.0232, and the mean is 2.8×10^{-3}. (b) For the spectral quality Q_s, the minimum is 0.1078, the maximum is 1.133, and the mean is 0.5830. (c) For the sphere reading quality Q_r, the minimum is 0.0068, the maximum is 573.2252, and the mean is 11.011.

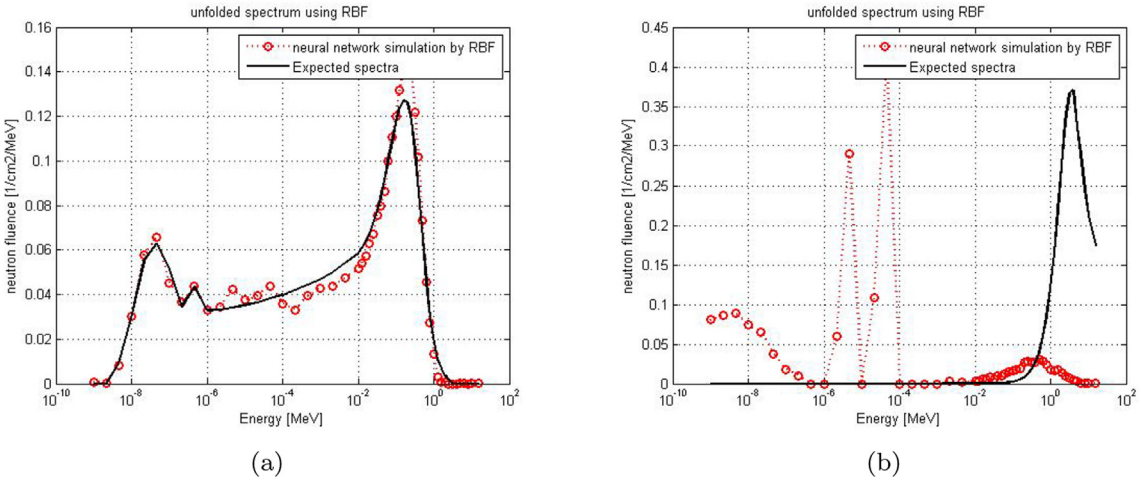

Fig. 8. (a) The best unfolded spectrum obtained by the radial basis function (RBF) method with solution space constraints (dotted red line) and the corresponding actual expected spectrum (continuous black line). (b) The worst unfolded spectrum (dotted red line) and the corresponding actual expected spectrum (continuous black line). (For interpretation of the references to colour in this figure legend, the reader is referred to the Web version of this article.)

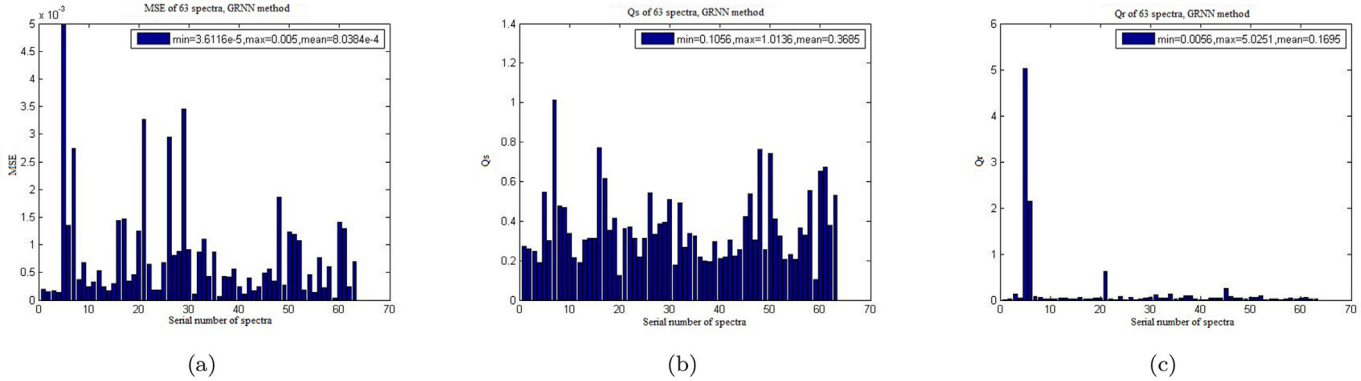

Fig. 9. Performance indexes of 63 spectra obtained by the generalized regression neural network (GRNN) method. (a) For the mean squared error (MSE), the minimum is 3.6116×10^{-5}, the maximum is 0.005, and the mean is 8.0384×10^{-4}. (b) For the spectral quality Q_s, the minimum is 0.1056, the maximum is 1.0136, and the mean is 0.3685. (c) For the sphere reading quality Q_r, the minimum is 0.0056, the maximum is 5.0251, and the mean is 0.1695.

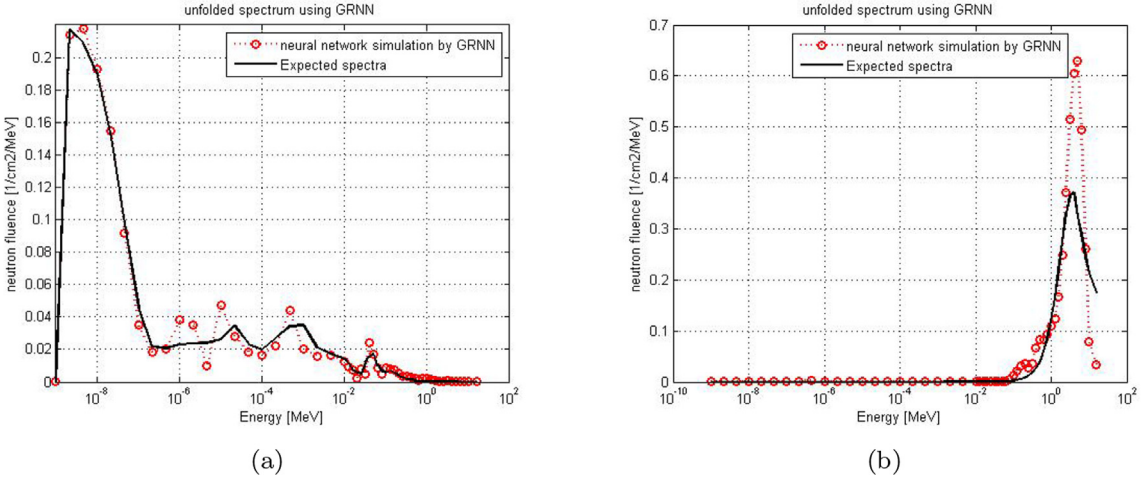

Fig. 10. (a) The best unfolded spectrum obtained by the generalized regression neural network (GRNN) method (dotted red line) and the corresponding actual expected spectrum (continuous black line). (b) The worst unfolded spectrum (dotted red line) and the corresponding actual expected spectrum (continuous black line). (For interpretation of the references to colour in this figure legend, the reader is referred to the Web version of this article.)

group. To assess the generalization ability, the mean values of the performance indexes MSE, Q_s, and Q_r were calculated and are given in the Table 1. The results show that the application of the multiseed averaging technique improves the performance. Fig. 5 shows the performance indexes of 63 spectra as bar graphs, from which the 24th is the best unfolded spectrum and the 7th is the worst unfolded spectrum according to Q_s. Fig. 6 shows the 24th and 7th unfolded spectra compared with the actual expected spectra. The best unfolded spectrum

matches well the expected spectrum, with MSE of 9.2311×10^{-5}, Q_s of 0.1567, and Q_r of 0.0138. The worst unfolded spectrum is not acceptable, with MSE of 3.7×10^{-3}, Q_s of 1.1711, and Q_r of 0.1727. The energy group corresponding to the peak of the nearly monoenergetic spectrum is not correct.

3.2. RBF neural network results

The RBF neural networks were tested for three optimum spread constants. Slight differences were found among the final results, and the performance was best when the spread constant was 0.15. However, the generalized unfolded spectra are not acceptable compared with the expected spectra: some negative values are present in the unfolded spectra, and the mean values of the performance indexes MSE, Q_s, and Q_r are relatively much larger. When solution space constraints as mentioned for the GA method were applied to the RBF neural networks, the unfolding performance greatly improved. The mean values of the performance indexes MSE, Q_s, and Q_r before and after use of space constraints are given in Table 2. Fig. 7 shows the performance indexes of 63 spectra as bar graphs obtained with RBF neural networks with solution space constraints, from which the 24th is the best unfolded spectrum and the 5th is the worst unfolded spectrum according to Q_s. Fig. 8 shows the best and the worst unfolded spectra compared with the actual expected spectra. The 24th spectrum matches the expected spectrum very well, with MSE of 4.364×10^{-5}, Q_s of 0.1078, and Q_r of 0.0068. However, the 5th unfolded spectrum, with MSE of 2.15×10^{-2}, Q_s of 1.133, and Q_r of 573.2252 is terrible compared with the expected highly monoenergetic neutron spectrum because of a lack of similarities with the spectra used in the training sets.

3.3. GRNN results

The GRNN method based on an optimum spread constant of 0.18 corresponding to the minimal mean value of the MSE had the best unfolding performance compared with the GRNN method based on other two optimum spread constants. Fig. 9 shows the performance indexes of 63 spectra as bar graphs obtained with the GRNN method, from which the 59th is the best unfolded spectrum and the 5th is the worst unfolded spectrum according to both the MSE and Q_r. Fig. 10 shows the best and the worst unfolded spectra compared with the actual expected spectra. The 59th unfolded spectrum matches perfectly with the expected spectrum, with MSE of 3.6116×10^{-5}, Q_s of 0.1056, and Q_r of 0.0235. The 5th unfolded spectrum, with MSE of 5×10^{3}, Q_s of 0.5453, and Q_r of 5.0251, is the worst but is still acceptable, the energy corresponding to the peak in the unfolded spectrum being the same as that of the actual expected spectrum, the only difference being the height. Compared with the GA and RBF neural network methods, the GRNN method is the most accurate method to unfold neutron spectra.

4. Discussion and conclusion

In this work, three different AI optimization methods were applied to unfold the same 63 neutron spectra randomly chosen from 251 spectra extracted from the IAEA compendium obtained with use of the response of a ^{3}He-filled Bonner sphere.

The solution space constraints, which are the combination of the eight-group scaling methods and semiempirical maximum determination from reference spectra, the cost, which consists of errors from sphere readings, the smoothness of the solution, and the difference between the unfolded spectrum and the reference spectrum, and the multiseed averaging technique modify the performance of the GA method for neutron spectrum unfolding. Compared with the GRNN method, the RBF method can automatically identify the repetition of spectrum samples in the training process. However, the generalized neutron unfolding performance of the RBF method is not acceptable. The application of the same solution space constrains as for the GA method in the RBF method can greatly improve the performance. The MSE can be used as a standard to optimize the spread constant of the RBF neural networks and GRNNs. The GRNN method requires the least time to preprocess and unfold neutron spectra and has the best performance and the most powerful generalization ability.

The GRNN method can be regarded as a fast, effective, accurate, and perfect method for neutron spectrum unfolding to obtain the neutron energy distribution online and off-line.

References

Alvar, A., Deevband, M., Ashtiyani, M., 2017. Neutron spectrum unfolding using radial basis function neural networks. Appl. Radiat. Isot. 129, 35–41.

Bedogni, R., Bortot, D., Buonomo, B., Esposito, A., Gomez-Ros, J., Introini, M., Lorenzoli, M., Pola, A., Sacco, D., 2014. First test of SP^{2}: a novel active neutron spectrometer condensing the functionality of Bonner spheres in a single moderator. Nucl. Instrum. Methods Phys. Res. Sect. A 767, 159–162.

Bedogni, R., Domingo, C., Esposito, A., Fernandez, F., 2007. FRUIT: an operational tool for multisphere neutron spectrometry in workplaces. Nucl. Instrum. Methods Phys. Res. Sect. A 580, 1301–1309.

Bedogni, R., Esposito, A., Gentile, A., Angelone, M., Gualdrini, G., 2008. Determination and validation of a response matrix for a passive Bonner sphere spectrometer based on gold foils. Radiat. Meas. 43, 1104–1107.

Braga, C., Dias, M., 2002. Application of neural networks for unfolding neutron spectra measured by means of Bonner spheres. Nucl. Instrum. Methods Phys. Res. Sect. A 476 (1), 252–255.

Bramblett, R., Ewing, R., Bonner, T., 1960. A new type of neutron spectrometer. Nucl. Instrum. Methods 9 (1), 1–12.

Freeman, D., Edwards, D., Bolon, A., 1999. Genetic algorithms- A new technique for solving the neutron spectrum unfolding problem. Nucl. Instrum. Methods Phys. Res. Sect. A 425, 549–576.

Frieden, B., 1988. Applications to optics and wave mechanics of the criterion of maximum Cramer-Rao bound. J. Mod. Opt. 35, 1297–1316.

Gomez-Ros, J., Bedogni, R., Moraleda, M., Delgado, A., Romero, A., Esposito, A., 2010. A multi-detector neutron spectrometer with nearly isotropic response for environmental and workplace monitoring. Nucl. Instrum. Methods Phys. Res. Sect. A 613, 127–133.

Gomez-Ros, J., Bedogni, R., Moraleda, M., Esposito, A., Pola, A., Introini, M., Mazzitelli, G., Quintieri, L., Buonomo, B., 2012. Designing an extended energy range single-sphere multi-detector neutron spectrometer. Nucl. Instrum. Methods Phys. Res. Sect. A 677, 4–9.

Hoshor, C., Oakes, T., Myers, E., Rogers, B., Currie, J., Young, S.M., C, J., Scott, P., Miller, W., Bellinger, S., Sobering, T., Fronk, R., Shultis, J., McGregor, D., Caruso, A., 2015. A portable and wide energy range semiconductor-based neutron spectrometer. Nucl. Instrum. Methods Phys. Res. Sect. A 803, 68–81.

Hsu, H., Alvar, K., Vasilik, D., 1994. A new Bonner-sphere set for high energy neutron measurements: Monte Carlo simulation. IEEE Trans. Nucl. Sci. 41, 938–940.

IEAE, 2001. Compendium of Neutron Spectra and Detector Response for Radiation Protection Purpose. Supplement to Technical Reports Series No. 318. IAEA Technical Report Series No. 403.

Jaynes, E., 1984. Prior information and ambiguity in inverse problems. SIAM-AMS Proc. 14, 151–166.

Kardan, M., Koohi-Fayegh, R., Setayeshi, S., Ghiassi-Nejad, M., 2004. Fast neutron spectra determination by threshold activation detectors using neural networks. Radiat. Meas. 38 (1), 185–191.

Kardan, M., Setayeshi, S., Koohi-Fayegh, R., Ghiassi-Nejad, M., 2003. Neutron spectra unfolding in Bonner sphere spectrometry using neural networks. Radiat. Prot. Dosim. 104 (1), 27–30.

Lis, M., Gomez-Ros, J., Bedogni, R., Delgado, A., 2008a. Design and feasibility of a multi-detector neutron spectrometer for radiation protection applications based on thermoluminescent ^{6}LiF:Ti,Mg (TLD-600) detectors. Nucl. Instrum. Methods Phys. Res. Sect. A 584, 196–203.

Lis, M., Gomez-Ros, J., Delgado, A., 2008b. Preliminary design of a single sphere multidetector directional neutron spectrometer using TLD-600. Radiat. Meas. 43, 1033–1037.

Mares, V., Schraube, H., 1994. Evaluation of the response matrix of a Bonner sphere spectrometer with LiI detector from thermal energy to 100 MeV. Nucl. Instrum. Methods Phys. Res. Sect. A 337, 461–473.

Martinez-Blanco, R., Ornelas-Vargas, G., Castaneda-Miranda, C., Solis-Sanchez, L., Castaneda-Miranada, R., Vega-Carrillo, H., Celaya-Padilla, J., Garza-Veloz, I., Martineez-Fierro, M., Ortiz-Rodriguez, J.M., 2016. A neutron spectrum unfolding code based on generalized regression artificial neural networks. Appl. Radiat. Isot. 117, 8–14.

Matzke, M., 2003. Unfolding procedures. Radiat. Prot. Dosim. 107, 155–174.

Mukherjee, B., 1999. Bondi-97: a novel neutron energy spectrum unfolding tool using a genetic algorithm. Nucl. Instrum. Methods Phys. Res. Sect. A 432, 305–312.

Reginatto, M., 2010. Overview of spectral unfolding techniques and uncertainty estimation. Radiat. Meas. 45, 1323–1329.

Reginatto, M., Goldhagen, P., Neumann, S., 2002. Spectrum unfolding sensitivity analysis and propagation on uncertainties with the maximum entropy deconvolution code MAXED. Nucl. Instrum. Methods Phys. Res. Sect.A 476, 242–246.

Routti, J., Sandberg, J., 1980. General purpose unfolding program LOUHI78 with linear

and nonlinear regularizations. Comput. Phys. Commun. 21 (1), 119–144.
Sanna, R., Brien, K., 1971. Monte Carlo unfolding of neutron spectra. Nucl. Instrum. Methods 91, 573–576.
Santos, J., Silva, E., Ferreira, T., Vilela, E., 2012. Unfolding neutron spectra obtained from BS-TLD system using genetic algorithm. Appl. Radiat. Isot. 71, 81–86.
Shahabinejad, H., Hosseini, S., Sohrabpour, M., 2016. Neutron spectrum unfolding using a two steps genetic algorithm. Nucl. Instrum. Methods Phys. Res. Sect. A 811, 82–93.
Shore, J., Johnson, R., 1980. Axiomatic derivation of the principle of maximum entropy and the principle of minimum cross entropy. IEEE Trans. Info. Theory 26 (1), 26–37.
Specht, D., 1991. A general regression neural network. IEEE Trans. Neural Netw. 2 (6), 568–576.
Suman, V., Sarkar, P., 2014. Neutron spectrum unfolding using genetic algorithm in a Monte Carlo simulation. Nucl. Instrum. Methods Phys. Res. Sect. A 737, 76–86.
Thomas, D., Alevra, A., 2002. Bonner sphere spectrometers—a critical review. Nucl. Instrum. Methods Phys. Res. Sect. A 476 (1), 12–20.
Toyokawa, H., Yoshizawa, M., Uritani, A., Mori, C., Takeda, N., Kudo, K., 1997. Performance of a spherical neutron counter for spectroscopy and dosimetry. IEEE Trans. Nucl. Sci. 44 (3), 788.
Vega-Carrillo, H., 2002. TLD pairs, as thermal neutron detector, in neutron multisphere spectrometry. Radiat. Meas. 35, 251–254.
Vega-Carrillo, H., Martinez-Blanco, M., Hernandez-Davila, Ortiz-Rodriguez, J., 2009. Spectra and dose with ANN of ^{252}Cf, ^{241}AmBe and ^{239}PuBe. Radioanal. Nucl. Chem 281 (3), 615–618.
Wiegerl, B., Alevra, A., Siebert, B., 1994. Calculations of the Response Function of Bonner Sphere with a Spherical ^{3}He Proportional Counter Using a Realistic Detector Model. Report PTB-N-21. Physikalisch-Technische Bundesanstalt, Braunschweig.
Yamaguchi, S., Uritani, A., Sakai, H., Mori, C., Iguchi, T., Toyokawa, H., Takeda, N., Kudo, K., 1999. Spherical neutron detector for space neutron measurement. Nucl. Instrum. Methods Phys. Res. Sect. A 422, 600–605.